

## Some Key Explorations in Planetary Rover Autonomy for ISRU Roles on the Moon

A. Ellery<sup>1</sup>

<sup>1</sup>Dept. of Mechanical and Aerospace Engineering, Carleton Univ., Ottawa, ON.  
Email: aellery@mae.carleton.ca

### ABSTRACT

We explore several facets of lunar rovers relevant to the conduct of lunar mining. In particular, we suggest that subsurface mining for asteroidal material shall be necessary. Our end-to-end 30 kg Kapvik microrover prototype has served as a testbed for exploring these issues—terramechanics, vision, SLAM, path planning, onboard intelligence, and multi-rover deployment. We suggest that microrovers are fully functionally capable platforms for lunar ISRU, especially if employed as cooperative fleets.

### INTRODUCTION

Most interest in in-situ resource utilisation (ISRU) lies in recovering water ice from the south pole but our interest is in recovering metals, glasses and ceramics from lunar minerals (Ellery 2020). For this, prospecting is required to determine stripping ratios (of waste to ore). We are concerned with the mining phase to recover minerals. Any form of excavation and hauling operations should be conducted as near autonomously as possible. Mining on Earth has a long history beginning with the acquisition of rocks to manufacture the first stone tools to the oldest underground mine (for haematite) in Swaziland dated to 40,000 y ago. The mining process typically involves drilling blastholes in rock, breaking rock into fragments by blasting, loading of broken ores by front loader or dragline and hauling by truck. Large-scale mining machines such as highwall mining machines are discarded from consideration as extraterrestrial mining for the foreseeable future will be small-scale. The main mining techniques include open pit, caving, bulk stoping, cut-and-fill and room-and-pillar. The lunar soil is suitable for extraction through surface mining. Open pit mining is conducted to recover near-surface resources typically through a series of descending benches. This type of mining is suited for the recovery of lunar regolith to access indigenous minerals. Open pit mining involves the extraction large amounts of useless overburden. Underground lunar mining are associated with affording radiation protection to human miners (Baiden et al 2010) but we anticipate roboticisation of mining. Exotic materials – nickel, cobalt, tungsten and selenium - may be sourced from impact craters exhibiting magnetic anomalies indicating the existence of impactor metals (Bland et al 2008). Underground mining will be essential for recovery of such non-indigenous meteoritic resources that are expected to be buried in the subsurface of shallow-angle craters (Collins 2012; Wieczorek et al 2012). Underground mining is characterised by their walls and roof supports (Hamrin 2001). Room-and-pillar mines excavate leaving a regular pattern of natural pillars in bedded ores to support the roof and walls. Within the mine for thick seams, excavation proceeds from the top downwards via benching in steps. The flat levels permit the use of wheeled front-end loaders and/or load-haul-dump vehicles. Stope-and-pillar mines are similar in combining room-and-pillar with cut-and-fill stoping. High quality ores are excavated around a random pattern of natural pillars of poor ores suited to suit more irregular ore bodies. The ores are mined in horizontal slices from the bottom-up and mined-out stopes are backfilled with tailings and sand. The vast majority of horizontal

deposits are mined using these two methods. For steeply dipping ore deposits, stoping involves mining from below the ore along the seam. In shrinkage stoping, ore is drilled and blasted from the ceiling and accumulates to form a platform. Ore is mined in horizontal slices but it is labour-intensive and unsuited to mechanisation. Sublevel stoping involves multiple regularly shaped stopes in the orebody in which holes are drilled and blasted. Automated load-haul-dumpers operated within open stopes which are backfilled after mining. These are unsupported mining approaches; supported mining methods are required in weak rock. Cut-and-fill stoping is the commonest supported method involving removing ore in horizontal slices from the bottom-up with mined-out stopes cement-backfilled as supports with any suitable waste material. It is adaptable to mining of steeply inclined and irregular deposits with selected ore pockets for which mechanised load-haul-dumpers are ideally suited. Caving involves controlled collapse of overlying ore in a large orebody without backfilling. Longwall mining is a caving method applicable to horizontal seams in which a long straight front wall is progressively undercut mechanically and caved back and forth along the face. A chain conveyor belts transport ore from the mine. Sublevel caving involves ore is blasted progressively downward through multiple levels connected by ramps in steeply inclined orebodies. Load-haul-dumpers excavate the blasted ores. Block caving is a bulk caving method in which large blocks of ore are undercut and fractured by blasting which are funnelled onto rail cars or more recently trackless load-haul-dumpers for transport. An important difference between terrestrial mines and prospective lunar mines will be scale. Terrestrial mines serve a huge global industry and market and are of an according scale. Extraterrestrial mines will serve a far more modest demand so will be on a far more diminutive scale. Whereas asteroid mining with microgravity environments will not require backfilling for stability after excavation, lunar mines are subjected to gravity conditions so backfilling may be required. Subsurface asteroidal ores may constitute combinations are large orebodies with more distributed ores. Now, surface rocks on the Moon are typically associated with young craters some of which may represent asteroidal material. Although the incidence of subsurface rocks (orebodies) is unknown, we may assume that their distribution may be similar to that on the surface. This suggests that mechanised cut-and-fill mining is most suited to underground lunar mining for accessing subsurface asteroidal ore resources.

There are also natural subsurface mines to other lunar resources. At diameters under 18 km on average (range 15–25 km), craters are simple excavations with a depth-to-diameter ratio,  $d/D$  of 0.14. Larger craters are more complex with flat floors and lower  $d/D$  ratio, wall terraces, central peaks and solidified impact melts within the crater. Still larger craters exceeding 300 km diameter exhibit concentric rings. More interestingly, skylights are partially collapsed cave ceilings forming cave entrances to subsurface lava tubes. Lava tubes are formed through flowing volcanic lava forming a crust as it cools through which hotter lava at the centre flows through and vacates its central core. Skylights have been identified on Mars in which cold trapping microclimates should have led to the accumulation of water ice (Cushing 2012). Similar skylights have been identified on the Moon. There are three well-studied lunar skylights at Mare Igenii, Mare Tranquillitatis and Marius Hills respectively with diameters ~50–100 m and depths ~40–100 m. It is possible that they, as cold traps, are repositories of water ice. Lava tubes also provide tunnel access to the subsurface. On the ground beneath the skylight, the terrain is likely to be rugged, littered with rubble from the collapsed ceiling. Lower gravity should yield significantly wider diameter lava tubes than on Earth suggesting that traverse through lava tubes can be ~several km. Kapvik is capable of abseiling down crater cliffs using tethers similar to cliffbot but while cliffbot adopted coordinated coordination with two anchorbots, Kapvik's wheels were freewheeling during tether-controlled descent and ascent (Mumm et al 2004;

Huntsberger et al 2007) (Fig 1a). Kapvik can be winched into a skylight from an anchored cable but there would not be the stability of an inclined cliff. Power and data can be transmitted from the surface through the tether terminating in a charging station.

## ROVER TERRAMECHANICS

Strip mining is based on rectilinear parallel strips in order to allow long conveyors to be used. This is not an efficient approach. A more efficient coverage strategy would be a spiral originating from the original position as the central base (Schmitt et al 1992). This affords an efficient areal coverage with minimum energy consumption. It does require a more complex navigation strategy than rectilinear coverage. There are various mobility systems that may be suited to the lunar terrain. One of the more sophisticated mobility concepts is the All-Terrain Hex-Limbed Extraterrestrial Explorer (ATHLETE) which employs six degree-of-freedom legs terminating in elastic wheels (tweels) (Heverly & Matthews 2008). For Kapvik, we adopted the six-wheeled rocker bogie system as a modular reference chassis for its flight heritage including Yutu-2 (Setterfield et al 2014) (Fig 1b). However, Kapvik was designed to accommodate different chassis modules and one such module is the elastic loop mobility system, a tracked chassis that offers high traction capability for challenging terrains (Ellery 2003) (Fig 1c).

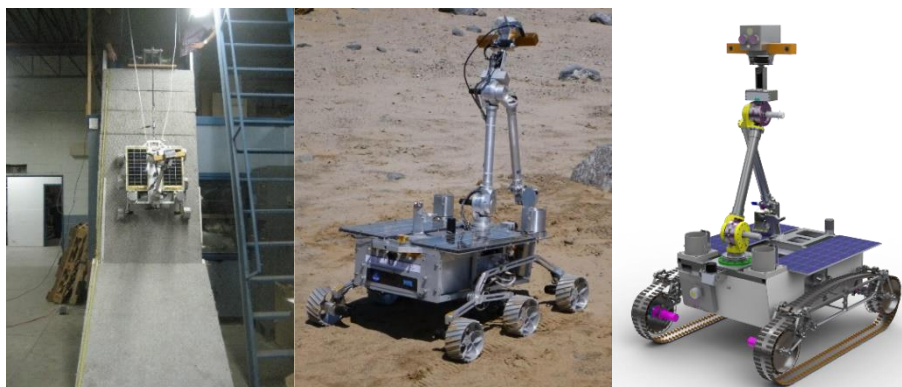


**Fig 1. (a) Kapvik abseiling a steep incline; (b) Kapvik with its rocker-bogie wheeled chassis undergoing trials at the CSA Mars Yard; (c) Kapvik with an elastic mobility system chassis for enhanced traction**

Drawbar pull is given by  $DP = H - R$  where  $H$ =soil thrust related to the Mohr-Coulomb equation for soil traction  $\tau = c + \sigma \tan \phi$ ,  $R$ =soil resistance dominated by compaction resistance due to wheel sinkage,  $c$ =soil cohesion,  $\phi$ =soil friction angle,  $\sigma$ =soil stress (Ellery 2005). Sinkage  $z$  is given by  $z = (\sigma/k)^{1/n}$  where  $k$ =pressure-sinkage coefficient,  $n$ =soil exponent. Sinkage may be estimated from wheel pressure  $p$  which determined from wheel loads measured by load cells above each wheel station of the rocker-bogie chassis – wheel load measurements are unique to Kapvik. From these measurements, a trained neural net model yields soil cohesion and friction angle estimates (Cross et al 2013) (Fig 2). Soil cohesion and friction measurement constitutes a type of tactile sensing of the soil.

Such continuous geotechnic measurements will be invaluable for siting lunar bases (Ellery 2021). In addition, drawbar pull of the rover may be estimated from the load measurements and traverse velocity to monitor rover traverse performance (Setterfield & Ellery 2013).

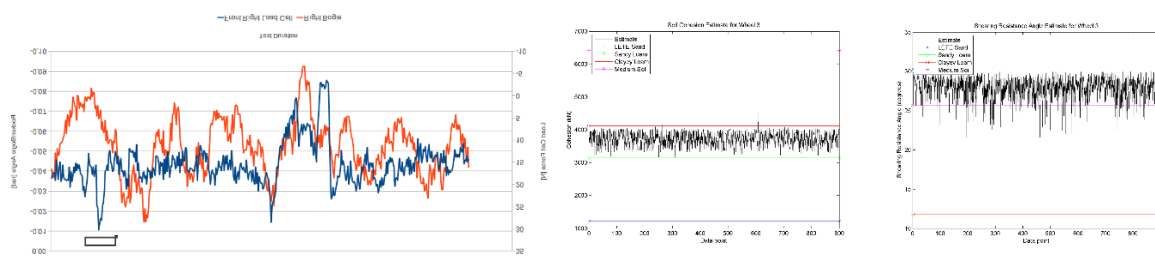


**Fig 2. Traverse of sandy-loam terrain at Petrie Island near Ottawa (a) wheel load measurements; (b) estimated soil cohesion; (c) estimated soil friction angle**

Planetary mining will require a mobile rover that digs, loads and hauls regolith or several rovers that are dedicated to digging/loading and hauling respectively. Digging regolith with an articulated arm-mounted backhoe is adequate for shallow depths but beyond 3m, a ripper blade will be required to loosen the compacted regolith. One approach to in-situ resource acquisition is random scooping of in-situ regolith. Another example of a random strategy would be a rotating bucket excavator used by the rover to scoop regolith onto an enclosed conveyor belt or hopper whilst traversing the terrain. A more focussed approach involves surveying to find specific in-situ resources. For example, a search for ilmenite deposits will require magnetometer surveys (Hay et al 2018) (Fig 3).

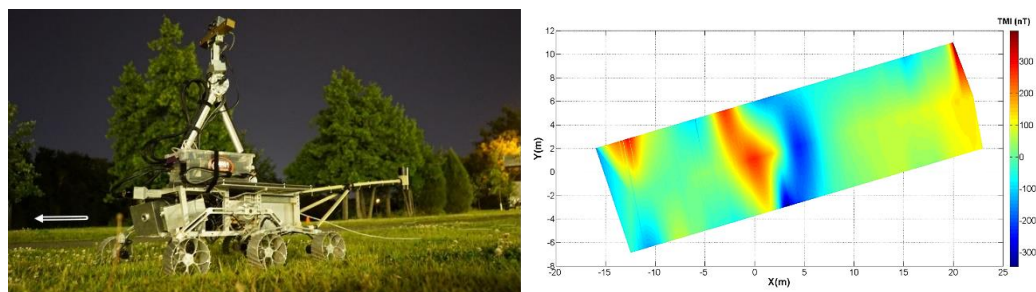


**Fig 3. (a) Kapvik microver equipped with boom-mounted magnetometer instrument; (b) scanned ground magnetic survey at the Carleton University campus**

Kapvik is configured with a soil scoop mounted at the end of a four degree-of-freedom manipulator similar to a JCB for acquiring regolith (Fig 4).



**Fig 4. Kapvik using its scoop to acquire regolith deposited into sample canisters**

More sophisticated regolith acquisition strategies may be explored by modelling front-loading excavation. For a soil-mover, the Mohr-Coulomb relation for computing the failure force due active (behind tool) and passive (in front of tool) earth pressure differences for digging is given by Reece earth-moving equation (Singh 1995):

$$F = F_p - F_a = \frac{1}{2} \gamma H^2 (K_p - K_a)$$

where  $K_{p,a}$ =passive/active force coefficients,  $\gamma=pg$ =specific density of soil,  $H$ =tool cut depth,

$$K_p = \frac{\sin^2(\alpha - \phi)}{\sin^2 \alpha \sin(\alpha + \delta) \left(1 - \sqrt{\frac{\sin(\phi + \delta) \sin(\phi + \beta)}{\sin(\alpha + \delta) \sin(\alpha + \beta)}}\right)^2}, \quad K_a = \frac{\sin^2((\pi - \alpha) + \phi)}{\sin^2(\pi - \alpha) \sin((\pi - \alpha) - \delta) \left(1 - \sqrt{\frac{\sin(\phi + \delta) \sin(\phi + \beta)}{\sin((\pi - \alpha) - \delta) \sin((\pi - \alpha) - \beta)}}\right)^2},$$

$\alpha$ =tool rake angle from horizontal,  $\beta$ =angle of soil surface,  $\phi$ =soil friction angle,  $\delta$ =soil-tool friction angle. Using Kapvik tool parameters and average lunar soil parameters (Table 1), the maximum tool digging force is given by Kapvik's lunar weight imposing a maximum tool cut depth of 17 cm.

**Table 1. Digging parameters**

Parameter	Symbol	Value
Soil density	$\rho$	1520 kg/m <sup>3</sup>
Soil cohesion	$c$	170 Pa
Soil friction angle	$\phi$	35°
Tool width	$b$	0.20 m
Tool cut height	$H$	
Tool rake angle of approach	$\alpha$	80°
Soil shear plane angle	$\beta$	45+ $\phi/2$
Soil-blade friction angle	$\delta$	$\phi/3$

## ROVER VISION

Any autonomous rover navigation system requires a vision system (DeSouza & Kak 2002). Kapvik is configured with a Point Grey Bumblebee colour stereo camera mounted onto a pan/tilt unit at the elbow of the four degree of freedom manipulator. Hence, the rover manipulator serves two functions – for directing a soil scoop and as the camera mast. This mounting provides an elevated panoramic camera field of view for autonomous navigation and with line of sight to the scoop during soil acquisition. In stereovision, the correspondence problem between the binocular images dominates the computational load through computation of sum-of-absolute-differences, sum-of-squared-differences or normalised-cross-correlation similarity (Tippets et al 2016). LIDAR range mapping offers a more reliable approach to 3D mapping and Kapvik employs a LIDAR scanner.

The Harris corner detector is not especially suited to extraterrestrial application until artificial structures with corners are constructed. However, feature-based descriptors search for specific features in images. Interest points may be selected by a difference of Gaussian to define salience which are matched with landmark estimates using feature descriptors. Speeded-up robust features (SURF) descriptors offer faster performance than scale-invariant feature transform (SIFT) descriptors. These keypoints represent blobs or corners in images rather than the Canny edge detector which uses Sobel filter masks. Binary robust independent elementary features (BRIEF) descriptors with reduced computational complexity permit previously-visited sites to be recognised even if that site undergone minor changes (Churchill & Newman

2013). Oriented BRIEF (ORB) is a variation on BRIEF. Random sample consensus (RANSAC) selects points randomly to estimate parameters of the plane and fits geometries to compute candidate rover poses with good outlier rejection (Lynen et al 2015). Iterative closest point (ICP) is used iteratively to match closest points of a point cloud over time from which target shapes can be extracted by fitting plane and shape primitives where Hough transforms are too computationally expensive. However, bundle adjustment (BA) derived from the maximum a posteriori (MAP) approach (as a form of abductive reasoning) for feature initialisation yields more accuracy than ICP. Object recognition and scene interpretation require further symbolic classification and labelling of objects and their relationships.

Vision is the basis for opportunistic scientific target selection and preliminary scientific analysis. Indeed, opportunistic science targets may be flexibly integrated into a rover traverse plan if the novelty of their visual features exceeds a threshold (Gallant et al 2013). To opportunistically search for scientific targets while traversing, the mast-mounted camera can pan-tilt similar to human active vision. There are two options: (i) optokinetic reflex is based on optic flow estimation of target motion via motion parallax information similar to visual odometry in hostile terrains; (ii) vestibular-ocular reflex is based on gyroscopic feedback measurements of head movement to control head movements. Rather than using camera-mounted gyroscopic feedback for pan-tilt control, pan-tilt motor displacement measurement feedback is augmented by mast-manipulator dynamic feedforward control (emulating cerebellar neural function) (Ross & Ellery 2017). Simulated on a Barratt arm, feedforward-augmented feedback control offers superior performance over feedback only control (Fig 5).

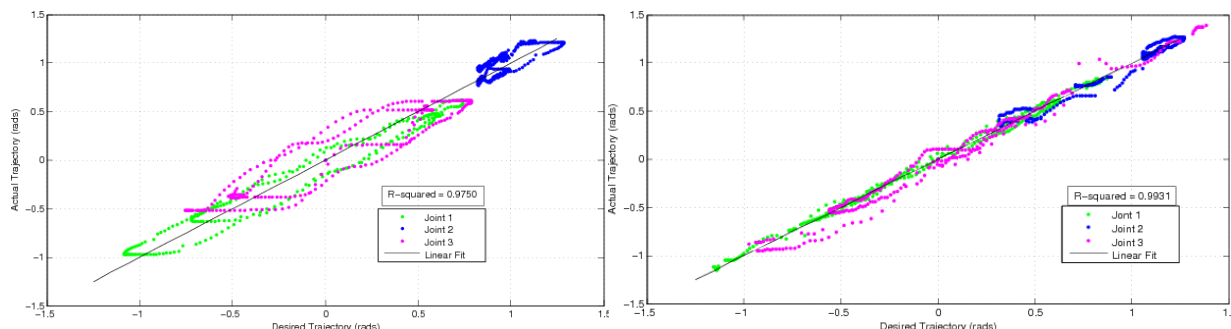


**Fig 5. Error excursion for 3 degree-of-freedom camera mast in tracking a moving object**  
**(a) feedback only; (b) feedforward-augmented feedback**

This provides the ability to search for and track moving targets during rover traverse. Such active stereovision incorporates visual “searchlight” of attention, gaze control and binocular vergence of the eyes to provide SIFT (salient) keypoints for object recognition (Aragon-Camarasa et al 2010).

Most space-rated processors have limited capabilities, e.g. ERC32, RAD series (such as the 200 MHz RAD750 on Curiosity) and LEON series processors. Although the real-time VxWorks operating system was used on the Mars rovers, we excluded it for Kapvik and adopted Linux with the Linux-compatible Player/Stage, the open-source predecessor to the robot operating system (ROS). We opted for FPGA-based Xiphos Q5 platforms for autonomous navigation algorithms with a commercial CAN bus protocols for its spaceflight heritage on Surrey satellites because SpaceWire was still under development at the time.

## SELF-LOCALISATION & MAPPING

An autonomous mining rover must negotiate significant obstacles (including terrain costs) and navigate within highly confined passageways. An occupancy grid map of cells, each labelled with a probabilistic Bayesian classification. Rather than dense grid-based maps, sparse sample-based maps representing maximum likelihood of the data points are an alternative (Meyer-Delius & Burgard 2010) but the former is well-established. A compromise might be to switch between dense occupancy and sparse feature-based map representations depending on the current observations (Wurm & et al 2010). Simultaneous localisation and mapping (SLAM) is the process of a rover locating itself within an environment represented in map form (Cadena et al 2016). Most approaches estimate rover pose with respect to a map of landmarks as the rover traverses. Feature locations in the environment are measured relative to the rover pose from which rover motion is estimated. Bayes theorem computes a posterior distribution:

$$p(x|z) = \frac{p(z|x)p(x)}{p(z)}$$

where  $p(x)$  is the prior (predicted) model,  $p(z|x)$  is the likelihood (observation/measurement) model and  $p(z)$  is empirical evidence. Bayesian inference through Bayes rule combines multiple sources of sensor data in a principled manner. Beliefs represent uncertainty as conditional probabilities. The Bayes filter estimates a system's probabilistic state (belief) representing uncertainty from noisy observations on the assumption of a Markovian process (Fox et al 2003). The Kalman filter is the commonest type of Bayes filter as the solution to the Riccati equation. The Kalman filter comprises a noisy predictive model, a noisy measurement model, an estimation of error covariances of both and a weighting mechanism (Kalman gain) that balances confidence in the model with that in the measurements. The Kalman filter may be employed for sensor fusion of odometry and external reference measurements (Marin et al 2013). State estimation involves estimating posterior probability  $p(x_{t+1}|z_t, u_t)$  of the rover pose subject to internal and environmental measurements through least square error minimisation methods such as Kalman and particle filters comprising a theoretical predictive Markovian model  $p(x_{t+1}|x_t, u_t)$  and an observation model  $p(z_t|x_t, m_t)$ , the back end and front end of SLAM respectively. A common approach is the use of the unscented Kalman filter to estimate the rover pose using odometry and external references to construct a digital occupancy grid map. The extended Kalman filter linearises a nonlinear model through a Taylor series expansion. Whereas the extended Kalman filter assumes Gaussian probability distributions fully described by mean and variance, e.g. (Lemaire et al 2007), the unscented Kalman filter samples nonlinearity with a set of sigma points. The Kalman filter is a special type of Bayesian navigation estimation (of posterior  $p(x_{i+1}|x_i, u_i)$ ) method describing predictive models and measurements (likelihood  $p(z|x)$ ) as probability density functions which includes particle filters (Durrant-Whyte 2001; Thrun 2002). Particle filters are sequential Monte Carlo methods that build a posterior probability based on a large number of random samples which are modified through model prediction and measurement update steps. Rao-Blackwellised particle filters for SLAM use particles as samples representing multiple rover trajectories and maps,  $p(x_{1:t}, m_j|z_{1:t}, u_{1:t-1})$  for large environments, e.g. (Sim et al 2007). Trajectory and landmark distribution may be modelled as a dynamic Bayesian network with the Markovian assumption to yield a posteriori estimates. Dynamic Bayesian networks are directed graphical models in each node is a random variable and each directed edge represents the conditional dependence between nodes. Similarly, a graphical approach to SLAM involves a graph of nodes corresponding to rover poses and landmarks over time with edges representing spatial constraints imposed by observations such as odometry (Grisetti et al 2010). GraphSLAM is a sparse view-based representation that

computes a maximum a posteriori (MAP) estimate of rover poses that minimises the negative log likelihood of all observations. A neural network can implement similar algorithms (Axenie & Conradt 2015). The SLAM graph represents a Gaussian Markov field that models the belief in the robot's pose. A directed Bayes tree equivalent to the square root information matrix is another graphical approach to SLAM (Kaess et al 2012). If there is no prior, MAP reduces to maximum likelihood estimation. However, incorporation of structured prior domain knowledge (such as that all objects are located on a common ground plane) into an object-based 3D SLAM process yields accurate predictions (Salas-Moreno et al 2013).

Data association (correspondence problem) is the matching current measurements with previous measurements in SLAM involving high computational complexity of computing the maximum likelihood of the fully correlated covariance matrix. The mean is required to compute the model Jacobian matrix while the covariance is required for generating data association hypotheses. The information matrix is the inverse of the covariance matrix with a sparse representation of correlations to reduce computational growth with the number of features of the map (Illa et al 2010). A 3D LIDAR scan on Kapvik was employed to generate noisy 3D point clouds in a discretised grid map, cells of which are classified in terms of traversability (Hewitt et al 2018). A neural network classifier trained by an extended Kalman filter performed the terrain classification given by  $w_{t+1} = w_t + K_t(y_t^d - h(x_t))$  where  $K_t = P_t H_t (1/\eta + H_t^T P_t H_t)^{-1}$ =Kalman gain and  $\eta = (H_t P_t H_t^T + R_t)^{-1} P_t$ =learning parameter. The Kalman filter exploits much more information than the backpropagation algorithm (Fig 6).

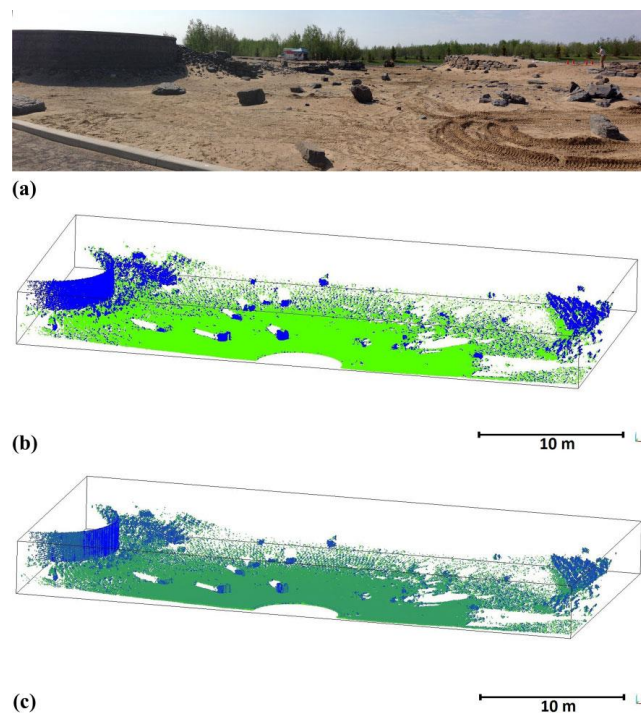


**Fig 6. CSA Mars Yard map (a) photograph; (b) binary classification; (c) graded classification**

In ISRU activities, rovers will explore new regions for the acquisition of resources but will return those resources to a base location from where it can be stored and/or utilised. Loop closure

(place recognition) involves determination that the rover has returned to a previously mapped location based on sensory observations of distinctive signatures (Leong & Newman 2006). Loop closure provides a means to reset any accumulated localisation errors implementing a balance between visiting new places (exploration) and prior-known places (exploitation). Place recognition is central to RatSLAM which generates topological maps of nodes as a continuous attractor network representing rover poses (Milford et al 2004; Lowry et al 2016). The hippocampus is a cognitive map for navigating both physical and social space (Eichenbaum 2015). Nodes are added if a new place is encountered or a previously-encountered place that has undergone major changes that render it unrecognisable. Visual homing is the process of computing the distance (sum of squared differences) between the snapshot image captured at the current pose of the rover and a snapshot image captured at the home target site (Szenher 2005). Compression of images into a 2D Haar wavelet transform signature may be used to quantify global similarity between images (enabling loop closure) facilitating SLAM on rovers with low computational resources (Pretto et al 2010). Place recognition is crucial in multi-rover environments.

## PATH PLANNING

Path planning as a predictive search for a temporal sequence of actions is a deliberative process (Ingrand & Ghallab 2017). The robot path planning problem may be defined as the robot traversing the environment from an initial pose to a final desired pose without interacting with intervening obstacles. The Piano Mover's Problem is the identical problem of moving furniture with a complex shape through a cluttered house of doorways, corridors and staircases. We can exhaustively test a series of every possible rigid-body transformations (translations and rotations) on the robot from the initial to final poses – this is the configuration (C-) space representation of pose configurations forming a Lie group through which a continuous freespace around obstacles must be defined (LaValle 2011). Although computationally NP-hard, certain assumptions (such as no rotations and shrinking the robot pose to a point) can reduce this substantially. In such cases, the A\* graph search algorithm can find a path through the C-space of rover poses (Thrun et al 2004). A more efficient approach with dynamic replanning capabilities by storing backpointers are variations of the D\* algorithm that find optimal paths in weighted occupancy grid maps (Dakulovic & Petrovic 2011). However, for navigating dynamic environments, D\* is inefficient in requiring extensive re-computations.

There is no doubt that integration of deliberative planning with reactive execution is highly desirable (Joyeux et al 2010). One way to achieve this is through the use of potential fields. An attractive potential is emplaced at the goal site while repulsive potentials are emplaced at each obstacle. The gradient of the sum of attractive and repulsive forces forces the rover to follow the potential minimum path to the goal while avoiding obstacles. Occupancy maps may be enhanced with virtual force fields in which each cell imposes potential forces (a sum of attractive forces for goals and repulsive forces for obstacles) on the rover. For example, place cells of a cognitive map may be used to generate a gradient (vector field) to a goal generated by 2D Gaussians over x and y coordinates (Fibla et 2010). A variation on the potential field is the fluid dynamics model in which the stream function is a gradient to the flow velocity field as a solution to the Laplace equation (Keymeulen & Decuyper 1994). The nonlinear viscoelastic potential field may have a modular form to represent limb forces generated by muscle groups, the vectorial superposition of which actuate limbs (Mussa-Ivaldi 1997). We initially adopted the Fajen-Warren polar

potential field (Hunang et al 2006) to examine path navigation through Mars rock distribution models as stringent highly rocky extraterrestrial environments (Golombek & Rapp 1997) (Fig 7). This particular potential field failed to find paths through the more extremely cluttered environments, namely the Mars Pathfinder landing site rock distribution (Mack & Ellery 2010) (Fig 7) but this is unrepresentative of the Moon.

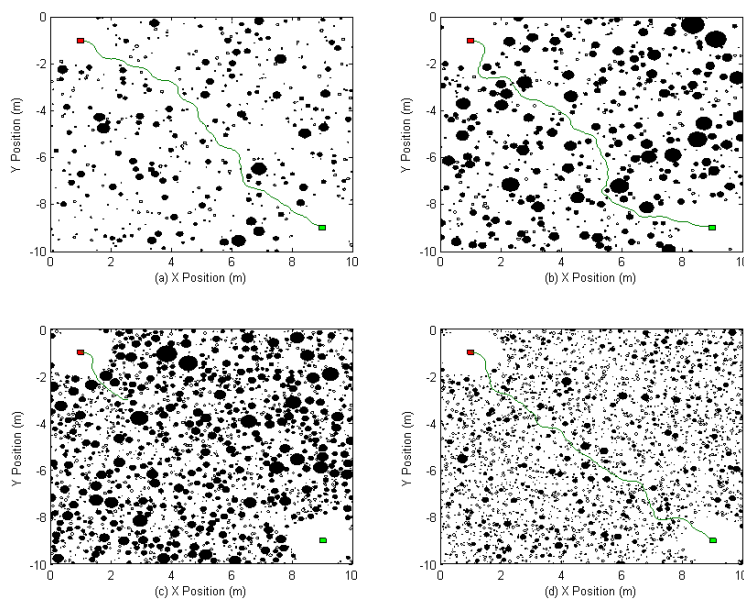


**Fig 7. Polar potential field generated paths through rock distributions at (a) Viking Lander 1 site; (b) Viking Lander 2 site; (c) Mars Pathfinder Lander site; (d) Mars Exploration Rover A landing site**

## ARTIFICIAL INTELLIGENCE AUGMENTATION

A semantic map incorporates semantic information about the environment into geometric and/or topological maps, effectively grounding it through sensorimotor interactions (Nuchter & Hertzberg 2008). Semantic information is richer than simple goal (attractor)-obstacle (repellor) classification in SLAM/path planning. Semantic information may be visual features that classify objects and their relationships as the basis of concepts (D'Este & Sammut 2008). Bayesian network classifiers can incorporate probabilistic semantic information into geometric or topological maps (Vasudevan & Siegwart 2008). Situation calculus is a logic for reasoning about the consequences (events) of actions. Dezert-Smarandache theory of plausible and paradoxical reasoning is a generalisation of Dempster-Shafer theory of evidence for selecting target of maximum interest based on an interest map (Ceriotti et al 2012). Dempster-Shafer theory and its variants are considerably more complex to compute than Bayesian inferencing. Fuzzy logic inferencing represents imprecision through fuzzy if-then rules used for feature classification: "IF  $x_1$  is  $C_{i1}$ ... AND  $x_{ij}$  is  $C_{ij}$  THEN object is  $C_i$ " (Tan et al 2005). High-level semantic knowledge is essential to permit the rover to interact and plan in its environment in a goal-directed manner (Galindo et al 2008; Galindo & Saffiotti 2013). Nevertheless, it is essential that symbols are grounded through sensorimotor interaction. We have explored an autonomous science system

based on Gabor filter processing of images of rocks followed by Bayesian network classification encoding scientific knowledge (Sharif et al 2015; Tettenborn & Ellery 2018; Arora et al 2017). A Bayesian network is a directed acyclic graphical knowledge structure representing the causal relationship between the nodes as conditional probabilities in the form:  $p(x_1, \dots, x_n) = \prod_{i=1}^n p(x_i | pa(x_i))$  where  $pa()$ =parental nodes. Large scale Bayesian network inferencing is NP-hard. Hidden Markov models (HMM) are a type of Bayesian network for which the Baum-Welch algorithm computes a maximum likelihood estimation of the HMM parameters using forward-backward computations.

## APPLICABILITY TO MULTI-ROVER SCENARIOS

The use of multiple robots offers significant advantages over single robots – they offer higher speedup, improved performance, higher reliability, greater adaptability and robustness. For enhanced cooperation between multiple robots, homogeneous team members are most efficient over heterogeneous team members (Waibel et al 2009). Multi-agent systems may be organised in hierarchies, holarchies, coalitions or markets (Horling & Lesser 2005). The market economy is a common mode of information sharing and coordination in multirobot systems (Yan et al 2013), e.g. sealed bid auctions for allocation of high-level tasks to different team members (Zlot et al 2002). Other paradigms are bio-inspired like “animat” approaches in which collective behaviour is an emergent property of interactions between individual agents such as social behaviour modelled by particle swarm optimisation (Doriya et al 2015). The methods used for single robots are directly applicable to multiple robots. Like for single rovers, multi-rover SLAM is based on Bayesian filters including Kalman filters, information filters, particle filters or neural networks with the additional requirement to exchange data between robots (Saeedi et al 2016). Kalman filter-based SLAM may be extended to multiple robots using occupancy grids explicitly communicated from multiple robots with covariances quantifying uncertainties (Zou & Tan 2013). The key challenge for multi-robot SLAM is data association between local maps of multiple robots fused into a global map. Line features such as the Hough transform may be used to align multiple maps (Vidal-Calleja et al 2011). The RANSAC algorithm is a common approach to map matching without communicating large amounts of data inherent in map representations. The sequential Bayesian filter estimates the state of the environment while following the gradient of mutual information to maximise joint measurement information between robots (Julian et al 2012). Maximising mutual information is equivalent to minimising conditional entropy,  $H(x_i | z_i) = H(x_i) - I(x_i, z_i)$  where  $I()$ =mutual information. Posterior estimation involves updating a weighted sample set through sequential importance resampling. A distributed expectation maximisation (EM) algorithm may be employed to generate a common reference frame with data association from error-prone measurements between multiple robots (Dong et al 2015). A greedy Bayesian approach can compute the probability of a specific rover moving to a specific neighbouring cell in its local map in the multi-robot area patrolling task (Portugal & Rocha 2013). Motor schema are potential field modules with specific reactive behaviours (move-to-goal – avoid-static-obstacle – avoid-robot - noise) that combine to form formation behaviours such as flocking in specific formation patterns (Balch & Arkin 1998): (i) obstacle avoidance to avoid crowding; (ii) gravitational cohesion to the centre of mass; (iii) goal-directed steering to average heading. The multi-robot implementation of behaviour control involves the addition of a single specialised avoid-robot module. Task-level behaviours may be added for fault tolerance – impatience behaviour (to complete tasks failed by others) and

acquiescence behaviour (to surrender its own failed task) (Parker 1998). A hybrid deliberative-reactive system comprises a reactive potential field system with deliberative waypoint-generating path planner (Gifford et al 2010). A set of modular behaviours (avoid-obstacle – attract-obstacle – avoid previous places – collision-response) generates a weighted composite behaviour. Waypoints are generated in a SLAM-generated occupancy grid-based map using a graph search algorithm. Mahalanobis, Manhattan or Euclidean distance quantifies the difference between individual robot maps. For example, weighted Euclidean distance is given by:

$d = \sqrt{\Delta x^T W^T W \Delta x}$ . Mean square error defines the Euclidean distance between an estimated and the true parameter value:

$$MSE = \frac{1}{T} \sum_{i=1}^T ((x_i - \hat{x}_i)^2 + (y_i - \hat{y}_i)^2)^2$$

Least squares algorithm is central to parameter estimation without prior information or measurement noise. Where the distance is minimum, multiple maps may be merged through averaging. In its recursive form, it may also incorporate a forgetting factor to weight data over time. Maximum likelihood may be used for parameter estimation if measurement noise is known.

## CONCLUSIONS

Commercial Lunar Payload Services (CLPS) landers are expected to provide scheduled lunar landers to the Moon's surface. In 2023, Astrobotic's Griffin lander is scheduled to deliver NASA's VIPER (Volatiles Investigating Polar Exploration Rover) carrying a mass spectrometer, neutron detector and near-infrared spectrometer for in-situ mapping of lunar water. Rovers will be required for ISRU prospecting and such rovers may be adapted to mining operations. We believe that microrover platforms such as Kapvik demonstrate that large rovers are unnecessary and inefficient. Microrovers have similar range and though their payload capacity is diminished, a multi-microrover approach eliminates this problem while introducing the prospect of distributed parallel exploration.

## REFERENCES

- Aragon-Camarasa G, Fattah H, Siebert P (2010) "Towards a unified visual framework in a binocular active robot vision system" *Robotics & Autonomous Systems* **58**, 276-286
- Arora A, Fitch R, Sukkarieh S (2017) "Approach to autonomous science by modelling geological knowledge in a Bayesian framework" *Proc IEEE/RSJ Int Conf Intelligent Robots & Systems*, Vancouver, Canada
- Axenie C, Conradt J (2015) "Cortically inspired sensor fusion network for mobile robot egomotion estimation" *Robotics & Automation* **71**, 69-82
- Baiden G, Grenier L, Blair B (2010) "Lunar underground mining and construction: a terrestrial vision enabling space exploration and commerce" *Proc 4th AIAA Aerospace Sciences Meeting Including the New Horizons Forum & Aerospace Exposition*, Orlando, FL
- Balch T, Arkin R (1998) "Behaviour-based formation control for multirobot teams" *IEEE Trans Robotics & Automation* **14** (6), 926-939
- Bland P, Artemieva N, Collins G, Bottke W, Bussey D, Joy K (2008) "Asteroids on the Moon: projectile survival during low velocity impacts" *39<sup>th</sup> Lunar & Planetary Science Conf*, abstract no 2045

- Cadena C, Carlone L, Carrillo H, Latf Y, Scaramuzza D, Neira J, Reid I, Leonard J (2016) "Past, present and future of simultaneous localization and mapping: toward the robust-perception age" *IEEE Trans Robotics* **32** (6), 1309-1332
- Ceriotti M, Vasile M, Giardini G, Massari M (2012) "Approach to model interest for a planetary rover through Dezert-Smarandache theory" *J Aerospace Computing Information & Communication* **5** (2), 1.37440
- Churchill W, Newman P (2013) "Experience-based navigation for long-term localisation" *Int J Robotics Research* **32** (14), 1645-1661
- Collins G (2012) "Moonstruck magnetism" *Science* **335**, 1176-1177
- Cross M, Ellery A, Qadi A (2013) "Estimating terrain parameters for a rigid wheeled rover using neural networks" *J Terramechanics* **50** (3), 165-174
- Cushing G (2012) "Candidate cave entrances on Mars" *J Cave & Karst Studies* **74** (1), 33-47
- D'Este C, Sammut C (2008) "Learning and generalizing semantic knowledge from object scenes" *Robotics & Autonomous Systems* **56**, 891-900
- Dakulovic M, Petrovic I (2011) "Two-way D\* algorithm for path planning and replanning" *Robotics & Autonomous Systems* **59**, 328-342
- DeSouza G, Kak A (2002) "Vision for mobile robot navigation: a survey" *IEEE Trans Pattern Analysis & Machine Intelligence* **24** (2), 237-267
- Dong J, Nelson E, Indelman V, Michael N, Dellaert F (2015) "Distributed real-time cooperative localization and mapping using an uncertainty-aware expectation maximization approach" *Proc IEEE Int Conf Robotics & Automation*, 5807-5814
- Doriya R, Mishra S, Gupta S (2015) "Brief survey and analysis of multi-robot communication and coordination" *Proc Int Conf Computing Communication & Automation*, 1014-1021
- Durrant-Whyte H (2001) "Critical review of the state-of-the-art in autonomous land vehicle systems and technology" *Sandia National Laboratories Report SAND2001-3685*, Albuquerque
- Eichenbaum H (2015) "Hippocampus as a cognitive map...of social space" *Neuron* **87**, 9-11
- Ellery A (2003) "Elastic loop mobility system (ELMS) study for Mars microrovers" Final Technical Report (ESA-Contract Number 16221/02/NL/MV), ESTEC Noordwijk, The Netherlands
- Ellery A (2005) "Robot-environment interaction - the basis for mobility in planetary microrovers" *Robotics & Autonomous Systems* **51**, 29-39
- Ellery A (2020) "Sustainable in-situ resource utilisation on the Moon" *Planetary & Space Science* **184**, 104870
- Ellery A (2021) "Leveraging in-situ resources for lunar base construction" in press with *Canadian J Civil Engineering*
- Fibla S, Bernadet U, Verschure P (2010) "Allostastic control for robot behaviour regulation: an extension to path planning" *Proc IEEE/RSJ Int Conf Intelligent Robots & Systems*, 1935-1942
- Fox D, Hightower J, Liao L, Schulz D, Borriello G (2003) "Bayesian filtering for location estimation" *Pervasive Computing* (Jul/Sep), 24-33
- Galindo C, Fernandez-Madrigal J-A, Gonzalez J, Saffiotti A (2008) "Robot task planning using semantic maps" *Robotics & Autonomous Systems* **56**, 955-966
- Galindo C, Saffiotti A (2013) "Inferring robot goals from violations of semantic knowledge" *Robotics & Autonomous Systems* **61**, 1131-1143

- Gallant M, Ellery A, Marshall J (2013) "Rover-based autonomous science by probabilistic identification and evaluation" *J Intelligent & Robotic Systems* **72** (3), 591-613
- Gifford C, Webb R, Bley J, Leung D, Calnon M, Makarewicz J, Banz B, Agah A (2010) "Novel low-cost, limited-resource approach to autonomous multi-robot exploration and mapping" *Robotics & Autonomous Systems* **58**, 186-202
- Golombek M, Rapp D (1997) "Size-frequency distributions of rocks on Mars and Earth analogue sites: implications for future landed missions" *J Geophysical Research* **102** (E2), 4117-4129
- Grisetti G, Kummerle R, Stachniss C, Burgard W (2010) "Tutorial on graph-based SLAM" *IEEE Intelligent Transportation Systems Magazine* (Winter), 31-43
- Hamrin H (2001) "Underground mining methods and applications" in *Underground Mining Methods: Engineering Fundamentals & International Case Studies* (ed. Hustrulid W, Bullock E) Society of Mining Metallurgy & Exploration Inc, 3-14
- Hay A, Samson C, Ellery A (2018) "Robotic magnetic mapping with the Kapvik planetary micro-rover" *Int J Astrobiology* 1-10. doi:10.1017/S1473550417000209
- Heverly M, Matthews J (2008) "Wheel-on-limb rover for lunar operations" *Proc 9<sup>th</sup> Int Symp Artificial Intelligence Robotics & Automation for Space*, Hollywood, USA
- Hewitt R, Ellery A, de Ruiter A (2018) "Training a terrain traversability classifier for a planetary rover through simulation" *Int J Advanced Robotic Systems* (Sep/Oct), 1-14
- Horling B, Lesser V (2005) Survey of multi-agent organizational paradigms" *Knowledge Engineering Review* **19** (4), 281-316
- Huang W, Fajen B, Fink J, Warren W (2006) "Visual navigation and obstacle avoidance using a steering potential function" *Robotics & Autonomous Systems* **54** (4), 288-299
- Huntsberger T, Stroupe A, Aghazarian H, Garrett M, Younse P, Powell M (2007) "TRESSA: teamed robots for exploration and science on steep areas" *J Field Robotics* **24** (11), 1015-1031
- Ila V, Porta J, Andrade-Cetto J (2010) "Information-based compact pose SLAM" *IEEE Trans Robotics* **26** (1), 78-93
- Ingrand F, Ghallab M (2017) "Deliberation for autonomous robots: a survey" *Artificial Intelligence* **247**, 10-44
- Joyeux S, Kirschner F, Lacroix S (2010) "Managing plans: integrating deliberation and reactive execution schemes" *Robotics & Autonomous Systems* **58**, 1057-1066
- Julian B, Angermann M, Schwager M, Rus D (2012) "Distributed robotic sensor networks: an information-theoretic approach" *Int J Robotics Research* **31** (10), 1134-1154
- Kaess M, Johannsson H, Roberts R, Ila V, Leonard J, Dellaert F (2012) "iSAM2: incremental smoothing and mapping using the Bayes tree" *Int J Robotics Research* **31** (2), 216-235
- Keymeulen D, Decuyper J (1994) "Fluid dynamics applied to mobile robot motion: the stream field method" *Proc IEEE Int Conf Robotics & Automation*, 378-385
- LaValle S (2011) "Motion planning: the essentials" *IEEE Robotics & Automation Magazine* **18** (1), 79-89
- Lemaire T, Berger C, Jung I-K, Lacroix S (2007) "Vision-based SLAM: stereo and monocular approaches" *Int J Computer Vision* **74** (3), 343-364
- Leong K, Newman P (2006) "Loop closure detection in SLAM by combining visual and spatial appearance" *Robotics & Autonomous Systems* **54**, 740-749
- Lowry S, Sunderhauf N, Newman P, Leonard J, Cox D, Corke P, Milford M (2016) "Visual place recognition: a survey" *IEEE Trans Robotics* **32** (1), 1-19

- Lynen S, Sattler T, Bosse M, Hesch J, Pollefey M, Siegwart R (2015) "Get out of my lab: large-scale, real-time visual-inertial localization" *Proc Robotics: Science & Systems*, Rome, Italy
- Mack A, Ellery A (2010) "The potential steering function and its application to planetary exploration rovers" *Proc 15th CASI Conf ASTRO*, Toronto
- Marin L, Valls M, Soriano A, Valera A, Albertos P (2013) "Multisensor fusion framework for indoor-outdoor localization of limited resource mobile robots" *Sensors* **13**, 14133-14160
- Meyer-Delius D, Burgard W (2010) "Maximum-likelihood sample-based maps for mobile robots" *Robotics & Autonomous Systems* **58**, 133-139
- Milford M, Wyeth G, Prasser D (2004) "RatSLAM: a hippocampal model for simultaneous localization and mapping" *Proc IEEE Int Conf Robotics & Automation* **1**, 403-408
- Mumm E, Farritor S, Pijanian P, Leger C, Schenker P (2004) "Planetary cliff descent using cooperative robots" *Autonomous Robots* **16**, 259-272
- Mussa-Ivaldi F (1997) "Nonlinear force fields: a distributed system of control primitives for representing and learning movements" *Proc IEEE Int Symp Computational Intelligence in Robotics & Automation: Towards New Computational Principles for Robotics & Automation*, Monterey, CA
- Nuchter A, Hertzberg J (2008) "Towards semantic maps for mobile robots" *Robotics & Autonomous Systems* **56**, 915-926
- Parker L (1998) "ALLIANCE: an architecture for fault tolerant multirobot cooperation" *IEEE Trans Robotics & Automation* **14** (2), 230-240
- Portugal D, Rocha R (2013) "Distributed multi-robot patrol: a scalable and fault-tolerant framework" *Robotics & Autonomous Systems* **61**, 1572-1587
- Pretto A, Menegatti E, Jiotsukawa Y, Ueda R, Arai T (2010) "Image similarity based on Discrete Wavelet Transform for robots with low computational resources" *Robotics & Autonomous Systems* **58**, 879-888
- Ross J & Ellery A (2017) "Panoramic camera tracking on planetary rovers using feedforward control" *Int J Advanced Robotic Systems* (May/Jun), 1-9
- Saeedi S, Trentini M, Seto M, Li H (2016) "Multiple robot simultaneous localization and mapping: a review" *J Field Robotics* **33** (1), 3-46
- Salas-Moreno R, Newcombe R, Strasdat H, Kelly P, Davidson A (2013) "SLAM++: simultaneous localization and mapping at the level of objects" *Proc IEEE Conf Computer Vision & Pattern Recognition*, 1352-1359
- Schmitt H, Kulcinski G, Sviatoslavsky I, Carrier W (1992) "Spiral mining for lunar volatiles" *Proc 3rd Int Conf Engineering, Construction & Operations in Space*, Denver, Co
- Setterfield T, Ellery A (2013) "Terrain response estimation using an instrumented rocker-bogie mobility system" *IEEE Trans Robotics* **29** (1), 172-188
- Setterfield T, Ellery A, Frazier C (2014) "Mechanical design and testing of an instrumented rocker-bogie mobility system for the Kapvik micro-rover" *J British Interplanetary Society* **67**, 96-104
- Sharif H, Samson C & Ellery A (2015) "Autonomous rock classification using Bayesian image analysis for rover-based planetary exploration" *Computers & Geosciences* **83**, 153-167
- Sim R, Elinas P, Little J (2007) "Study of the Rao-Blackwellised particle filter for efficient and accurate vision-based SLAM" *Int J Computer Vision* **74** (3), 303-318

- Singh S (1995) "Learning to predict resistive forces during robotic excavation" *IEEE Int Conf Robotics & Automation*, 2102-2107
- Szenher M (2005) "Visual homing in natural environments" *Proc Towards Autonomous Robotics*, 221-228
- Tan K, Chen Y, Wang L, Liu D (2005) "Intelligent sensor fusion and learning for autonomous robot navigation" *Applied Artificial Intelligence* **19**, 433-456
- Tettenborn A & Ellery A (2018) "Comparison of Gabor filters and wavelet transform methods for extraction of lithological features" *Proc Int Symp Artificial Intelligence Robotics & Automation in Space*, Madrid, Spain, paper no. P9
- Thrun S (2002) "Probabilistic robotics" *Communications of ACM* **45** (1), 51-57
- Thrun S, Thayer S, Whittaker W, Baker C, Burgard W, Ferguson D, Hahnel D, Montemerlo M, Morris A, Omohundro Z, Reverte C, Whittaker W (2004) "Autonomous exploration and mapping of abandoned mines" *IEEE Robotics & Automation Magazine* (Dec), 79-94
- Tippetts B, Lee J, Lillywhite K, Archibald J (2016) "Review of stereo vision algorithms and their suitability for resource-limited systems" *J Real-Time Image Processing* **11**, 5-25
- Vasudevan S, Siegwart R (2008) "Bayesian space conceptualization and place classification for semantic maps in mobile robotics" *Robotics & Autonomous Systems* **56**, 522-537
- Vidal-Calleja T, Berger C, Sola J, Lacroix S (2011) "Large scale multiple robot visual mapping with heterogeneous landmarks in semi-structured terrain" *Robotics & Autonomous Systems* **59**, 654-674
- Waibel M, Keller L, Floreano D (2009) "Genetic team composition and level of selection in the evolution of cooperation" *IEEE Trans Evolutionary Computation* **13** (3), 648-660
- Wieczorek M, Weiss B, Steart S (2012) "Impactor origin for lunar magnetic anomalies" *Science* **335**, 1212-1215
- Wurm K, Stachniss C, Grisetti G (2010) "Bridging the gap between feature and grid-based SLAM" *Robotics & Autonomous Systems* **58**, 140-148
- Yan Z, Jouandeau N., Chreif A (2013) "Survey and analysis of multi-robot coordination" *Int J Advanced Robotic Systems* **10**, 399
- Zlot R, Stenyz A, Dias B, Thayer S (2002) "Multi-robot exploration controlled by a market economy" *Proc IEEE Int Conf Robotics & Automation*, 3016-3023
- Zou D, Tan P (2013) "CoSLAM: collaborative visual SLAM in dynamic environments" *IEEE Trans Pattern Analysis & Machine Intelligence* **35** (2), 354-366